



A specific inflammatory suppression fibroblast subpopulation characterized by MHCII expression in human dilated cardiomyopathy

Xi Fan¹ · Kai Huang¹ · Yuming Wu² · Sheng Jin² · Liewen Pang¹ · Yiqing Wang¹ · Bo Jin³ · Xiaotian Sun¹

Received: 25 September 2023 / Accepted: 12 January 2024

© The Author(s), under exclusive licence to Springer Science+Business Media, LLC, part of Springer Nature 2024

Abstract

Dilated cardiomyopathy (DCM) is a significant cause of heart failure that requires heart transplantation. Fibroblasts play a central role in the fibro-inflammatory microenvironment of DCM. However, their cellular heterogeneity and interaction with immune cells have not been well identified. An integrative analysis was conducted on single-cell RNA sequencing (ScRNA-Seq) data from human left ventricle tissues, which comprised 4 hearts from healthy donors and 6 hearts with DCM. The specific antigen-presenting fibroblast (apFB) was explored as a subtype of fibroblasts characterized by expressing MHCII genes, the existence of which was confirmed by immunofluorescence staining of 3 cardiac tissues from DCM patients with severe heart failure. apFB highly expressed the genes that response to IFN- γ , and it also have a high activity of the JAK-STAT pathway and the transcription factor RFX5. In addition, the analysis of intercellular communication between apFBs and CD4⁺T cells revealed that the anti-inflammatory ligand-receptor pairs TGFB-TGFR, CLEC2B-KLRB1, and CD46-JAG1 were upregulated in DCM. The apFB signature exhibited a positive correlation with immunosuppression and demonstrated diagnostic and prognostic value when evaluated using a bulk RNA dataset comprising 166 donors and 166 DCM samples. In conclusion, the present study identified a novel subpopulation of fibroblasts that specifically expresses MHCII-encoding genes. This specific apFBs can suppress the inflammation occurring in DCM. Our findings further elucidate the composition of the fibro-inflammatory microenvironment in DCM, and provide a novel therapeutic target.

Keywords Fibroblast heterogeneity · Single-cell RNA sequencing · Inflammation · Dilated cardiomyopathy

Introduction

Heart failure (HF) is a progressive disease characterized by decreased systolic or diastolic function of the heart. It is one of the leading causes of death in developed countries, affecting over 60 million people worldwide [1]. Dilated

cardiomyopathy (DCM) is the most common disease in HF [2]. The occurrence and progression of DCM are associated with complicated pathophysiological processes, including inflammation and fibrosis, which ultimately lead to ventricular remodeling [3].

Fibroblasts are crucial to fibrosis and chronic inflammation, which can modulate inflammatory cells by secreting cytokines such as IL-1 β , INF- γ , TNF- α , and CCL5 [4, 5]. Meanwhile, immune cells including macrophages and T cells can influence the activation and extracellular matrix (ECM) production of fibroblasts [6, 7]. Dysregulation of the fibro-inflammatory microenvironment, which is composed of fibroblasts, immune cells, cytokines and ECM, plays a central role in pathological process of DCM [8].

Thanks to the expanding applications of single-cell RNA sequencing technology, the heterogeneity of fibroblasts has raised increasing interest recently [9, 10]. Various subpopulations of fibroblasts, including myofibroblasts, ECM-producing fibroblasts, as well as immune-associated fibroblasts, have been identified [9, 11]. These subpopulations contribute

✉ Yiqing Wang
wangyiqing@huashan.org.cn

✉ Bo Jin
jinbo7711@aliyun.com

✉ Xiaotian Sun
drsunxiaotian@126.com

¹ Department of Cardiothoracic Surgery, Huashan Hospital of Fudan University, 12 Wulumuqi Rd, Shanghai 200040, China

² Department of Physiology, Hebei Medical University, Shijiazhuang, China

³ Department of Cardiology, Huashan Hospital of Fudan University, 12 Wulumuqi Rd, Shanghai 200040, China

prominently to cardiac reconstruction and inflammation in HF. And notably, a cancer-associated subpopulation of fibroblasts with antigen-presenting functions has been identified in tumors [12, 13], and has been involved in the modulation of the immune microenvironment. However, whether a similar subpopulation of fibroblasts regulating inflammatory immunity exists in DCM remains unknown.

Herein, we integrated two adult human cardiac ScRNA-Seq datasets (GSE145154 and GSE183852) to explore the heterogeneity of cardiac fibroblasts in DCM. We successfully identified a specific subpopulation named antigen-presenting fibroblasts (apFBs)—whose existence was validated by human heart tissues—with an immunosuppressive function via modulating CD4⁺ T cells, and we also validated this result using an external, independent bulk RNA sequencing (bulk RNA-Seq) dataset (GSE141910).

Materials and methods

Patient selection and tissue collection

The study was approved by the ethics committee of Huashan Hospital [ethical approvals: KY2017-323]. All patients received a written informed consent for tissue donation, which specified the purpose of the study. We obtained left ventricular tissues from 3 explanted hearts of patients with DCM who were undergoing heart transplantation. Before immunostaining, samples were fixed in 4% buffered formalin for 48 h and then embedded in paraffin.

Datasets

ScRNA-Seq data of ten human left ventricular tissues were downloaded from gene expression omnibus (GEO; GSE145154 [8] and GSE183852 [14]) including 4 healthy donor hearts and 6 DCM hearts with severe heart failure. In the former dataset (containing tissues from one healthy donor and two DCM patient sources), samples from each patient were sequenced after CD45⁺ and CD45⁻ flow sorting separately, performing excellently in the abundance of immune cells; The latter ScRNA-seq dataset contains two healthy donors and five DCM patients. 332 individual DCM samples were selected from the bulk RNA-Seq dataset (GEO; GSE141910) that enrolled in the study.

ScRNA-seq data analysis

Quality control

All analyses were based on R (V.4.1.3) (<https://www.r-project.org/>). A Seurat object was created by importing the sample

matrices into the Seurat (V.4.1.1) R package. The percentage of mitochondrial genes, ribosomal genes and erythroid genes were calculated separately using the PercentageFeatureSet function in Seurat. Filter cells used the following conditions: (1) $800 < nCount\ RNA < 10,000$; (2) $500 < nFeature$; (3) mitochondrial reads $< 10\%$; (4) erythrocyte reads $< 1\%$. Cells that pass the appeal quality control were preserved and utilized for subsequent analyses.

Batch correction and cell cluster

For the saved object, normalization was performed using NormalizeData with default settings, and variable features were calculated by FindVariableFeatures function (“vst” method). Then, the data was scaled utilizing ScaleData with default settings, and the principal components were calculated by RunPCA (npcs set to 35). The number of PCs was chosen by visualizing a plot with the “ElbowPlot” function. Harmony (V.0.1.0) [15] was used to remove batch effects from the datasets. Seurat’s FindClusters function was used to cluster cells, run multiple times over a range of resolution parameters (0.1–1). The appropriate resolution was selected via comparing cluster results by R package Clustree (V0.5.0) [16]. The “RunUMAP” function was used for the visualization. All cell populations were annotated using known markers. Cells expressing multiple cell type markers were considered to be hybrid cells and these cells were not analyzed subsequently.

Recluster of fibroblast and T cell

Extracted the fibroblast and T cell to form a new seurat object, respectively. Each data were normalized, variable features calculated (nfeatures set to 2000 for fibroblasts and 1000 for T cells), scaled, and principal components calculated (npcs set to 20 for fibroblasts and 25 for T cells). The RunHarmony function was run with default settings. After the batch correction, clusters were calculated by the FindNeighbors function (reduction based on harmony, dimensions set to 1: npc) and FindClusters function (Louvain algorithm, resolution set to 0.2 for fibroblasts and 0.8 for T cells). For fibroblasts, the marker genes of each subpopulation were calculated using the FindAllMarker function (“MAST” method) [17], min.pct was set to 0.3 and logfc.threshold was also set to 0.3. The calculated marker genes and their functional enrichment results were used to annotate the fibroblast subpopulations. For T cell subclusters, recognized markers were used to annotation.

Differential gene expression and gene set enrichment analysis (GSEA)

Cluster-specific differential expression genes (DEGs) between donors and DCMs were identified utilizing the

FindMarkers function with the following settings: test = MAST, min.pct = 0.3, logfc.threshold = 0.3. The DEGs with adjusted p value < 0.05 were included in further analysis. GSEA based on marker genes and DEGs was performed by gProfiler2 (V.0.2.1) [18]. The gost function run with the default settings. After removing ribosomal genes in advance, only the gene lists remaining more than five genes after P value adjustment were tested. Only the terms from GO [19], Reactome [20] and KEGG [21] were plotted.

Gene scores

Enrichment scores were calculated by Seurat function “AddModuleScore” (setting the number of control features to 100). The ECM gene sets were obtained from the matrixome project [22]. GO terms for fibroblast proliferation, activation, and antigen processing and presentation were GO: 0048144, GO: 0072537, and GO: 0019882.

Activity of transcription factors and signal pathways

Transcription factor activity was estimated for each cell by viper (V.1.28.0) [23] based on transcription factors from DoRothEA (V.1.6.0) [24]. The R package PROGENy (V.1.16.0) was used to assess the signaling pathway activity of each cell and summarize the score of each subpopulation for each group. For pseudobulk, Seurat's AverageExpression function was used with default parameters. For each subpopulation, scores were summarized and the most variable transcription factors were plotted.

Ligand-receptor mediated intercellular communication

The R package CellChat (V.1.4.0) [25] was used for comparative analysis between groups of cell–cell communication. We selected “secrete autocrine/paracrine signaling” and “cell–cell contact” interactions from cellchatDB in analysis.

Data processing of bulk RNA-seq and analysis

The bulk RNA-Seq data was mapped by STAR [26], and the read was counted by featureCounts function. The assessment of the associations among apFBs signature gene expression levels was conducted utilizing Spearman correlation coefficients. The receiver operating characteristic (ROC) curves were generated to evaluate the diagnostic value of the signature genes of apFBs. The random forest algorithm was used for ranking the importance of prognosis-related genes. Risk score models containing sex, age and top 3 prognosis-related genes were constructed for prognosis prediction.

Immunofluorescence in human tissues

5- μ m-thick sections of paraffin-embedded tissues were evaluated by double immunofluorescence analysis. The sections were incubated in 5% bovine serum albumin in PBS after dewaxed and rehydrated. Primary antibodies (PDGFR α , Abcam, # ab203491; HLA-DRB1, Abcam, # ab133578) at 1: 100 dilution were incubated overnight at 4 °C. Then, sections were incubated with fluorescent secondary antibody (ABflo™ 488-conjugated Goat Anti-Rabbit IgG, ABclonal, #AS039; ABflo™ 594-conjugated Goat Anti-Rabbit IgG, ABclonal, #AS053) at 1:150 dilution for 1 h at 25 °C. DAPI was used for nuclear counterstaining. Sectioning images were taken using confocal microscope (Olympus, IX37) and analyzed by ImageJ software.

Statistics

A students' two-tailed unpaired t test was used to determine the significance of the difference between two groups; Two-way ANOVA was used among more than three independent groups. If normal-distribution or equal-variance assumptions were not valid, statistical significance was evaluated using the Mann–Whitney test and the Wilcoxon signed rank test. Statistical analysis was conducted using GraphPad Prism (V.8.0.2). For GSEA, Hypergeometric test was used followed by multiple comparison correction. The method of correction for gProlifer2 was performed by g:SCS algorithm [27], which was developed by the authors of the gProfileR package. P values < 0.05 were considered to be significant.

Results

Overview of the cell composition of the human left ventricle

We collected 85,827 single cells from two datasets of seven patients with DCM and three donors. Of these cells, 81,595 passed the stringent quality control filters and were further divided into populations of C0–C18 at a resolution of 0.4 (Figure S1A, S1B). No sample-specific variation existed within each cluster (Figure S2A). Low-quality cells individually clustered into one cluster were excluded (Figure S2C). C11, C12, C17, and C18 were identified as hybrid cells due to their expression of markers of multiple cell types, and were excluded from further analysis (Figure S2D).

The entire population was classified into 11 major cell types based on their respective molecular features (Fig. 1A, B). These cell types were presented in both donor and DCM hearts (Fig. 1C). C0 and C10, with high expression levels of DCN, FBLN1, and LUM, were defined as fibroblasts ($n = 27,237$); endothelial cells (C1, C6, and C9; $n = 17,181$)

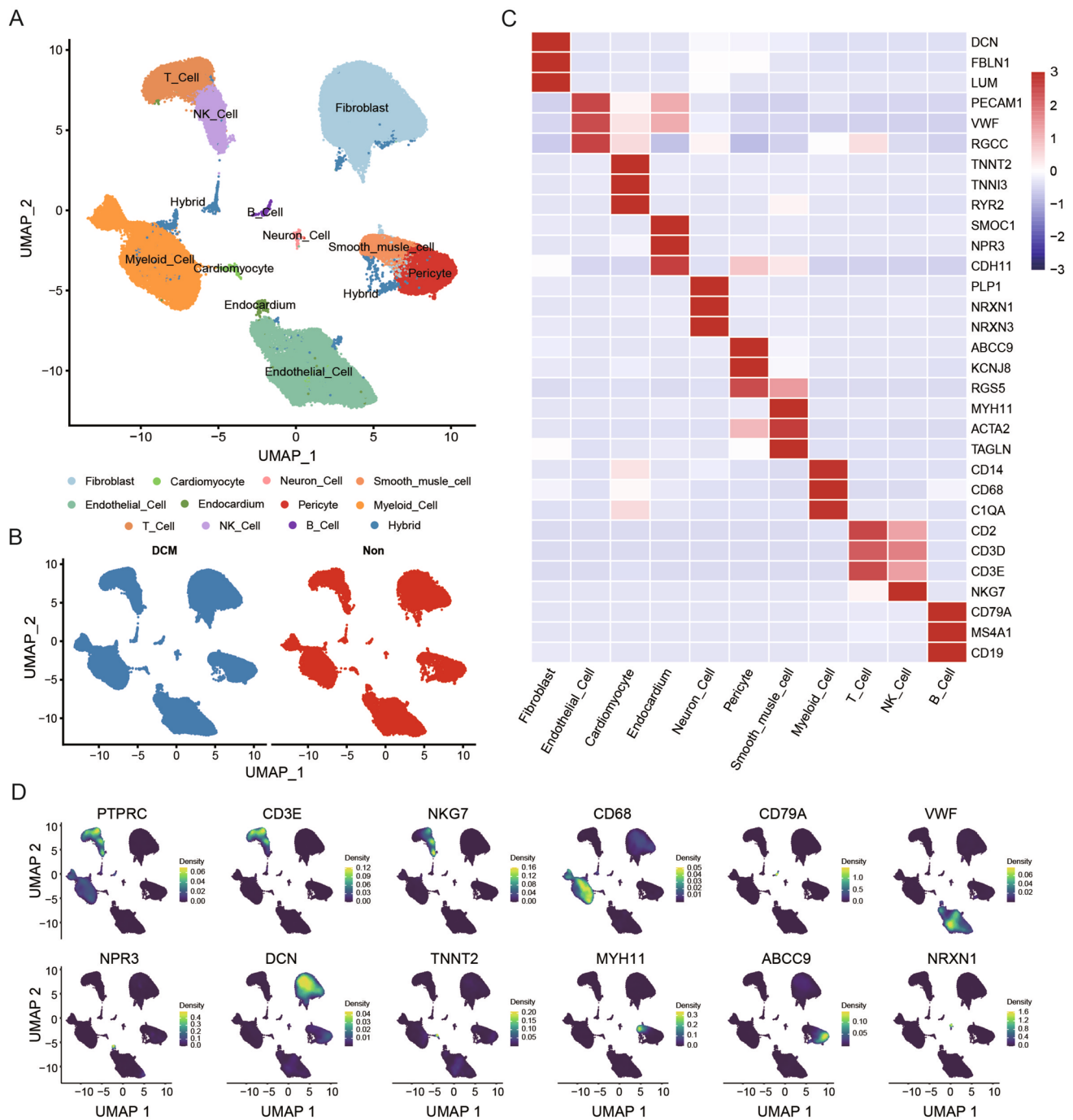


Fig. 1 Cell atlas of the human heart. **A** Graph-based clustering of 81,595 cells with UMAP based on the integration of two ScRNA-seq datasets. **B** UMAP split by different conditions (with and without

DCM). **C** Heatmap of the known markers expressed in each cell type. **D** Density plots of selected marker genes, illustrating their expression patterns

were identified by the pan-EC markers, PECAM1, VWF, and RGCC. C4 cells were identified as pericytes due to the specific expression of ABCC9 and KCNJ8 ($n=6750$); ACTA2, TAGLN, and MYH11 were enriched in C7 cells as smooth muscle cells ($n=2190$). We identified immune cells by PTPRC expression and further defined T cells by

CD2 and CD3 expression ($n=6932$), NK cells by NKG7 expression ($n=3929$), myeloid cells by CD68 expression ($n=14,294$), and B cells by CD79A expression ($n=443$); some endocardial cells (NPR3, SMOC1; $n=422$) and neural cells (NRXN1, NRXN3; $n=371$) were also identified. Little cardiomyocytes (C16; $n=309$) marked by TNNT2, TNNI3,

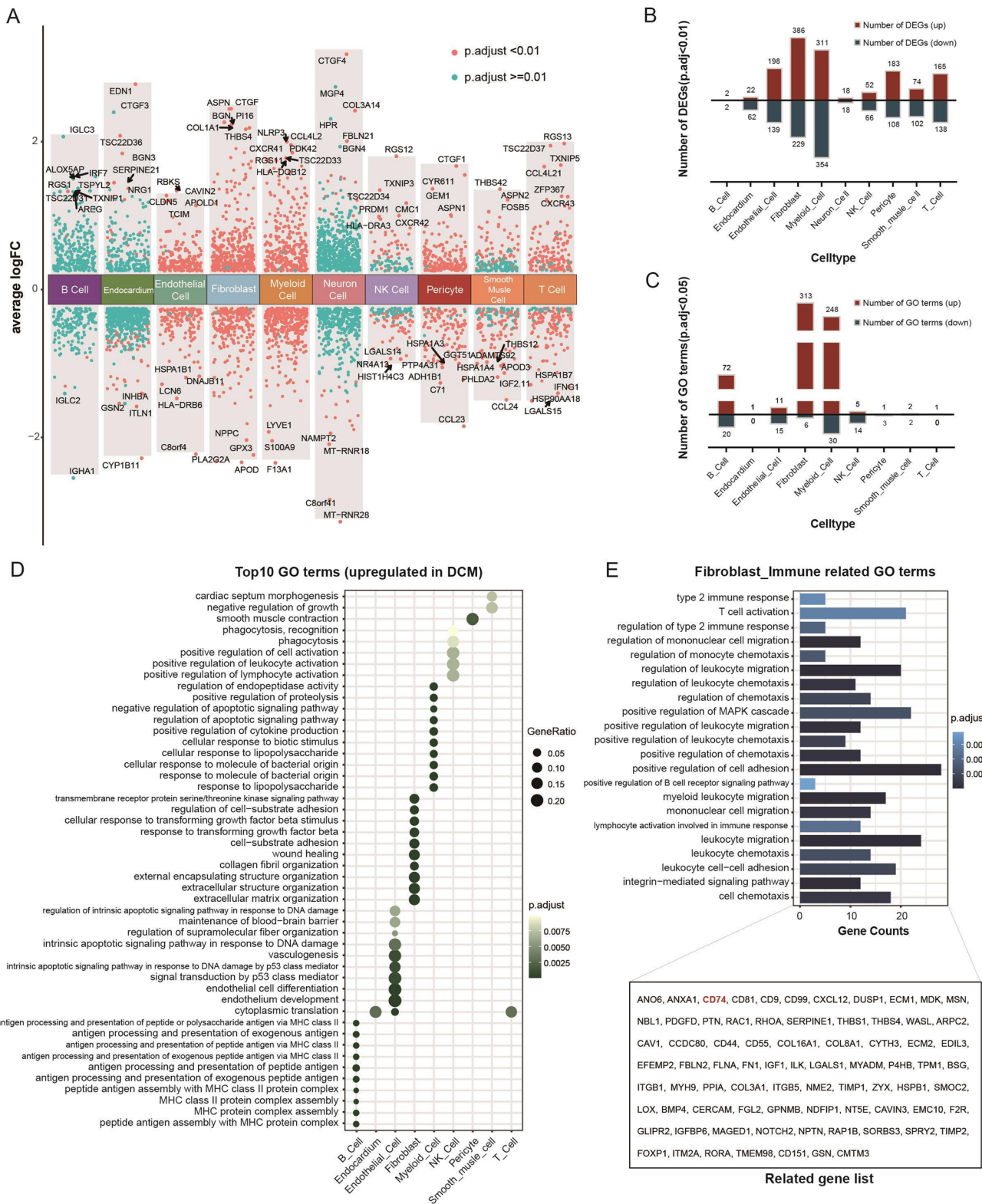


Fig. 2 Differential gene analysis and functional enrichment of non-cardiomyocytes. **A** Differential gene expression analysis showing the up- and down-regulated genes across all populations. An adjusted p value of <0.01 is indicated in red, while an adjusted p value of ≥0.01 is indicated in blue. **B** The number of DEGs with an adjusted p value of <0.01 across all populations. Up- and down-regulated genes are

shown as red and green bars, respectively. **C** The number of enriched GO terms with an adjusted p value of <0.05. Up- and down-regulated genes are shown as red and green bars, respectively. **D** Top 10 GO terms for upregulated DEGs of each cell type. **E** The upregulated DEGs of fibroblasts in DCM-enriched GO terms related to immune regulation. The box shows the genes associated with the GO terms

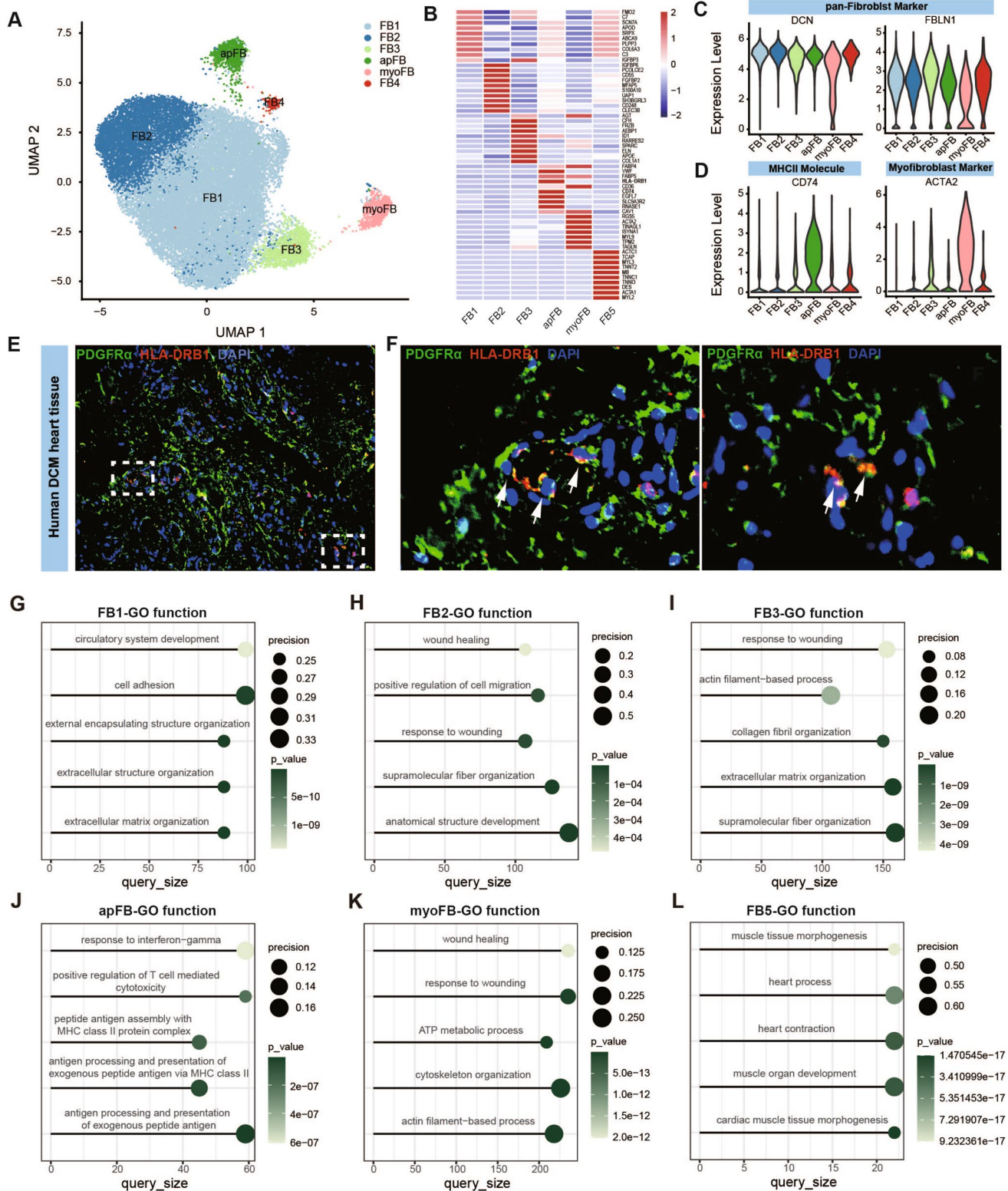


Fig. 3 Characteristics of fibroblast subpopulations. **A** UMAP depicting subtypes of fibroblast. **B** Heatmap of calculated marker genes expressed by fibroblast subtypes. **C** Violin plot showing Pan-marker expression of fibroblasts for each subcluster. **D** Violin plot of CD74 and ACTA2 expression level per cluster. **E**, **F** Tissues from DCM

patients were subjected to Dual-color fluorescence staining for apFBs (PDGFR α ⁺HLA-DRB1⁺). The boxed region in (**E**) indicates the section as in (**F**). PDGFR α (green), HLA-DRB1 (red), DAPI (blue). **G**–**L** Gene sets enriched in marker genes per fibroblast subtype. Dot size refers to the overlap of the tested genes per the gene set (precision)

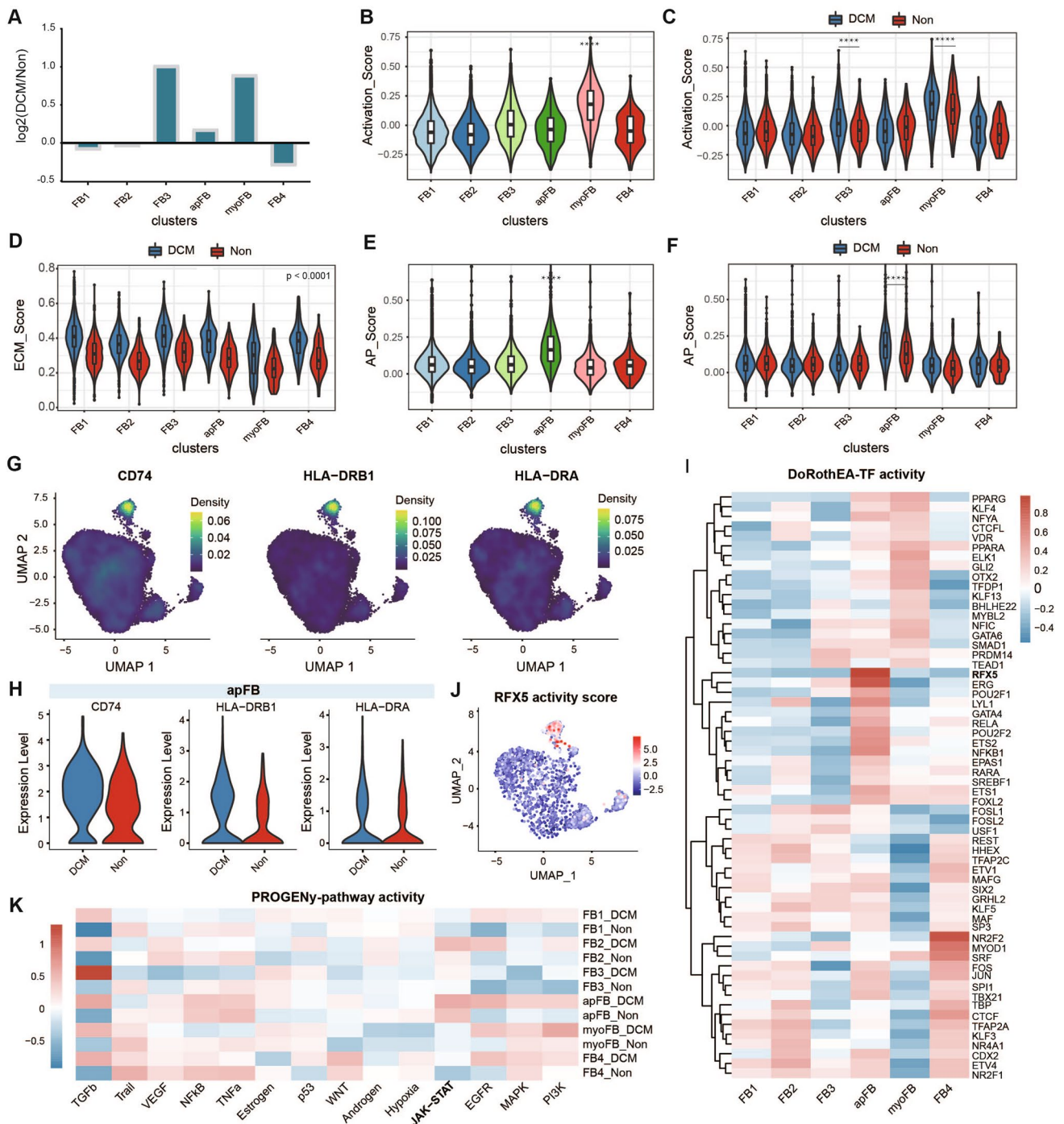


Fig. 4 Distribution and expression characteristics changes of fibroblast subpopulations and intrinsic drivers of MHCII gene expression. **A** Ratio changes of cell clusters in DCM versus donor heart. **B, C** Violin plot of fibroblast activation scores per cluster and condition. **D** Violin plot of ECM scores per cluster and condition. **E, F** Violin plot of antigen presentation scores per cluster and condition. ***p < 0.0001, two-sided unpaired Wilcoxon rank sum test. **G** Den-

sity map of gene expression levels of MHCII molecules in apFB. **H** Violin plot of gene expression levels of MHC molecules in apFB per condition. **I** Prediction of transcription factor (TF) activity of each fibroblast subpopulation based on TF regulons (DoRothEA). **J** UMAP plots of RFX5 activity scores. **K** Prediction of signal pathway activity of each fibroblast subpopulation based on pathway-responsive genes (PROGENy)

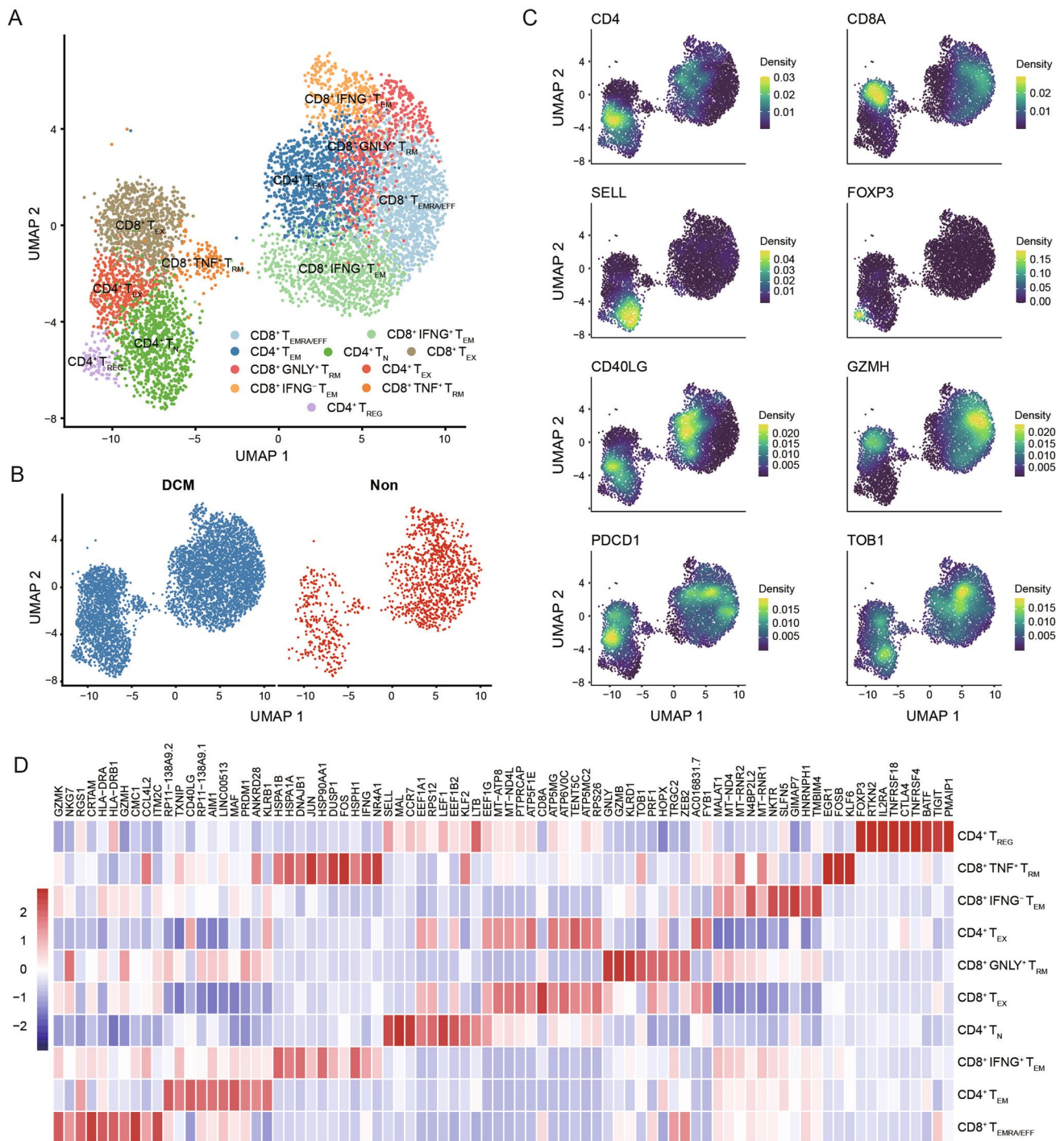


Fig. 5 T cell subpopulations. **A** UMAP depicting subtypes of T cell. **B** UMAP split according to different conditions. **C** Density plot of known marker expression levels in T cell subtypes. **D** Heatmap of calculated marker genes expressed by T cell subtype

and RYR2 were obtained because of the limitation of capturing by 10X platform, so they were not included in the subsequent analysis. The distribution of the cells expressing characteristic markers was shown in Fig. 1D.

Fibroblasts present the most transcriptional alterations in DCM

To explore the DCM-related genes, we analyzed the differentially expressed genes (DEGs) of each cell type between the donor and DCM hearts. Extensive transcriptional alterations

were observed among all populations (Fig. 2A, complete list presented in Table S1). Endothelial cells, fibroblasts, myeloid cells, pericytes, and T cells appeared to manifest more substantial changes during HF (Fig. 2A, B). Fibroblasts exhibited the most DCM-associated transcriptomic changes compared with other cell types (Fig. 2B, C).

Functional enrichment analysis of fibroblasts revealed aberrant production of ECM and collagen fibers in DCM, which is consistent with previous findings that fibroblasts contribute to structural remodeling in HF (Fig. 2D). In line with this, COL1A1, PI16, and THBS4—the top 3 upregulated genes—were related to collagen production, fibroblast proliferation, and injury-associated extracellular matrix production. The upregulated genes in endothelial cells were significantly enriched in vasculogenesis, endothelial cell differentiation, endothelium development, and the intrinsic apoptotic signaling pathway in response to DNA damage mediated by p53. The immune cells exhibited pro-inflammatory features in DCM: Macrophages exhibited enhanced phagocytosis and promoted cytokine production; and NK cells upregulated the expression of genes involved in phagocytosis, recognition, and positive regulation of leukocyte activation (Fig. 2D).

Fibroblasts exhibit enhanced immunomodulatory features in DCM

The immune-related genes of fibroblasts upregulated in DCM and their enriched functions were examined. The results demonstrated that fibroblasts exhibited many transcriptional changes associated with regulating the immune microenvironment, including promoting leukocyte adhesion, enhancing the recruitment of immune cells, regulating the production of various cytokines by immune cells, and activating immune cells via the MAPK cascade pathway (Fig. 2E).

The immune-related genes expressed by fibroblasts upregulated under the condition of DCM were further investigated (Fig. 2F). CD74—a protein-encoding gene associated with class II major histocompatibility complex (MHCII)—regulates antigen presentation for immune response. This unexpected finding suggests that a particular subpopulation of fibroblasts expressing MHCII molecules can deliver antigens and participate in the remodeling of the immune microenvironment. To confirm this finding, we reclustered the fibroblast population.

Reclustering of fibroblasts and antigen-presenting fibroblasts (apFBs) expressing MHCII molecules presented in the human heart

Fibroblasts were extracted to recluster, and six subclusters were identified at a resolution of 0.2 (Fig. 3A). The expression levels of the pan-Fibroblast marker were examined

for all subpopulations, and all subpopulations exhibited high expression levels of DCN and FBLN1 (Fig. 3C). FB1 expressed COL6A3 encoding the alpha-3 chain (one of the three alpha chains of type VI collagen) (Fig. 3B), whose main functions were cell adhesion and ECM production (Fig. 3G). FB2 specifically expressed high levels of PCOLCE2—enabling collagen binding activity (Fig. 3B), which was involved in anatomical structure development and the response to wounding (Fig. 3H). COL1A1 and APOE were highly expressed in FB3 and were associated with type I collagen production and inflammation promotion (Fig. 3B). FB3 was a major class of injury responsive, ECM producing, collagen fiber, and polymer fiber producing subclusters that may contribute substantially to structural remodeling in DCM (Fig. 3I). However, FB4 was highly expressed in several genes encoding myosin with the function of cardiac morphogenesis and development (Fig. 3L). Besides, we also identified myofibroblasts (myoFB), which specifically expressed ACTA2 and the proliferation-related gene RGS5 (Fig. 3B, D). The results of GO enrichment revealed the function of wound healing and actin filament-based processes in myoFB (Fig. 3L). The complete list of calculated marker genes in enriched GO terms is presented in Table S2.

Notably, a subcluster specifically expressing genes encoding MHC class II molecules (CD74, HLA-DRB1) was identified and annotated as apFB (Fig. 3B). Colocalization of PDGFR α , a membrane-localized specific marker protein of cardiac fibroblasts, and HLA-DRB1 confirmed the presence of apFBs in human hearts (Fig. 3E, F). The functional enrichment results indicated that apFBs could process and present antigens via MHCII and interact with T cells. Furthermore, apFBs exhibited a response to IFN- γ (Fig. 3J), suggesting a potential mechanism for the acquisition of its antigen-presenting phenotype, as IFN- γ is a common inducer of MHCII expression in non-antigen-presenting cells.

Expression of MHCII molecules by apFBs may be mediated by transcription factor RFX5 and JAK-STAT pathway in response to IFN- γ

Fibroblast proliferation, activation, and ECM production play a central role in the progression of HF. The distribution and expression level of characteristic gene sets were examined. FB3 and myoFB were significantly increased in DCM (Fig. 4A). Examination of the activity scores among the subpopulations revealed higher scores in FB3 and myoFB, and the scores further increased in DCM, especially myoFB (Fig. 4B, C). Regarding ECM production, the scores of all subpopulations were significantly increased in DCM (Fig. 4D).

We then explored the antigen processing and presentation scores of individual subpopulations. apFB exhibited the highest scores, whereas other cell types consistently

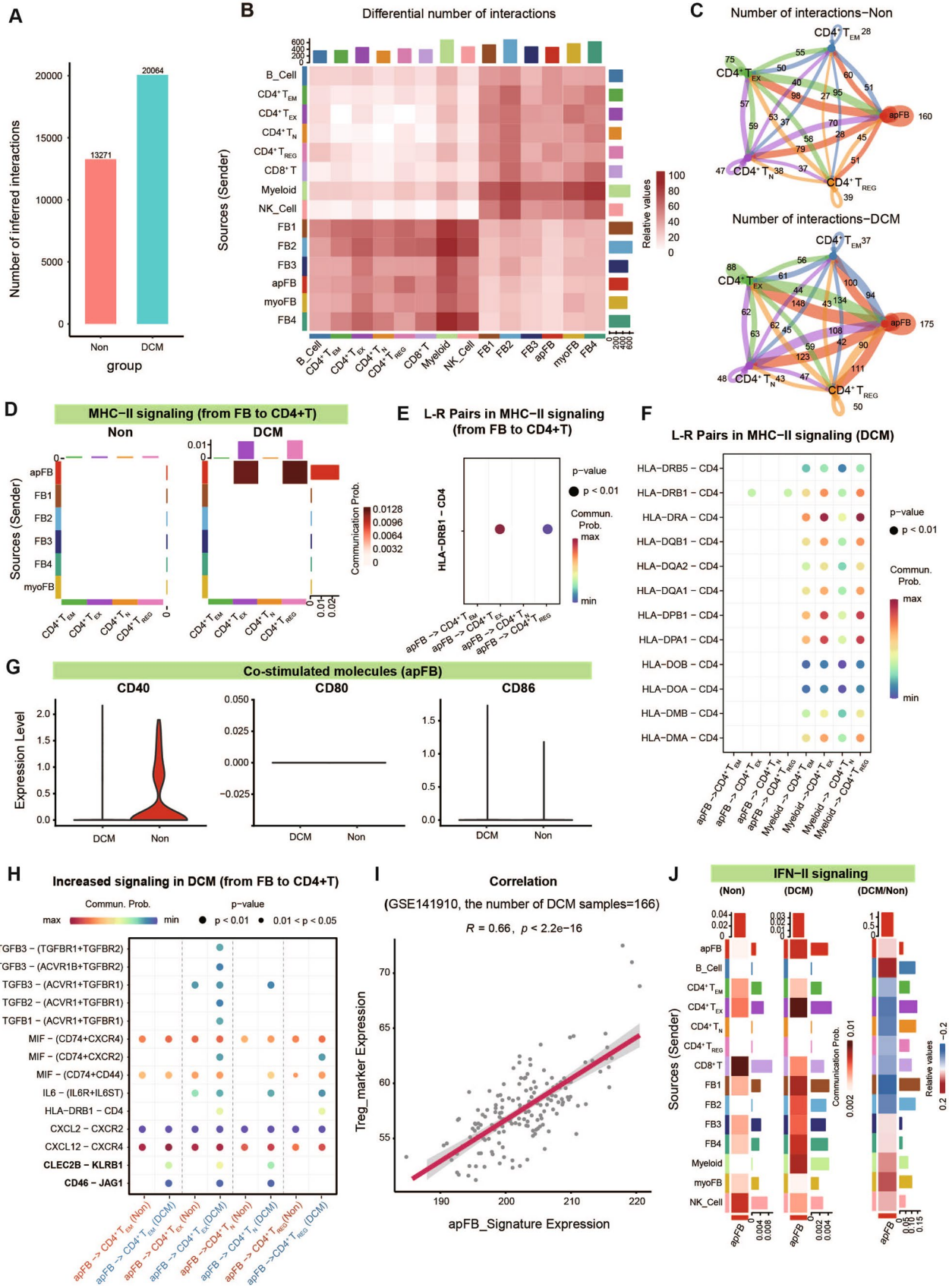


Fig. 6 Altered fibroblast-immune cell crosstalk and perturbation of CD4⁺T by apFB in DCM. **A** Number of inferred interactions between fibroblasts and immune cells per condition. **B** Heatmap of the differential number of inferred interactions between fibroblasts and immune cell subpopulations (DCM versus Non). **C** Circle chart of inferred interaction number between apFB and CD4⁺T subpopulations for each condition. **D** Heatmap of communication probabilities for MHCII signaling pathways. **E** Dot plot of L-R pairs in MHCII signaling, with apFB as the signal sender and CD4⁺T subpopulation as the receiver. **F** Dot plot of L-R pairs in MHCII signaling. **G** Violin plot of co-stimulated molecule gene expression levels in apFB per condition. **H** Dot plot of L-R pairs of upregulated signaling in DCM from apFB to CD4⁺T cell. **I** correlation analysis between apFB and T_{reg}. **J** Left heatmap of IFN-II signal communication probability from other populations to apFBs, split according to different conditions. Right: heatmap of differential communication probability of IFN-II signaling from other populations to apFB (DCM versus Non)

exhibited lower scores (Fig. 4E). In DCM, the antigen presentation scores of apFB were further increased, whereas those for other cell types remained unchanged (Fig. 4F).

The expression of genes encoding MHCII molecules (CD74, HLA-DRB1, and HLA-DRA) in fibroblast subclusters was examined. These genes were specifically highly expressed by apFB (Fig. 4G), and the expression level was increased under DCM (Fig. 4H). To reveal the intrinsic factors driving the different functional lineage of fibroblasts, we calculated the transcription factor activity of each cell. RFX5—a protein-encoding gene—was the highest active transcription factor in apFBs, which can activate the transcription of MHCII by recognizing and binding the X1 box of their promoters (Fig. 4I, J). Furthermore, the pathway activity of each cell type exhibited a higher activity of the JAK-STAT pathway in apFBs that induced MHCII molecules expression in response to IFN- γ [28] (Fig. 4K).

T cell subpopulation identification and characterization

As apFBs expressed genes encoding MHCII molecules, this class of fibroblast may have potential interactions with CD4⁺T cells. To investigate this finding, we reclustered the T cells.

The TOP1000 HVG with a resolution of 0.8 was selected to recluster the T cells, and 10 subpopulations were identified based on known markers (Fig. 5A, C). An increasing distribution of T cells was observed in DCM (Fig. 5B). The expression of CD4 and CD8 was used to identify CD4⁺T cells and CD8⁺T cells; SELL was used to identify naive T cells (T_N); FOXP3 was used to identify CD4⁺regulatory T cells (T_{reg}). CD40LG was one of the CD4⁺effector memory cell markers (T_{EM}), whereas recently activated effector CD8⁺memory cells/effector T cells (T_{RAEM/EFF}) expressed high levels of GZMH [29]. Tissue-resident memory T cells

(T_{RM}) were characterized by TOB1 expression [30], whereas exhausted T cells (T_{EX}) expressed high levels of PDCD1 [31]. The calculated marker genes for each subcluster are shown in Fig. 5D. T_{EM} was divided into IFN⁺T_{EM} and IFN⁻T_{EM} according to the expression of IFN, and T_{RM} was classified into TNF⁺T_{RM} and GNLY⁺T_{RM} according to their expression characteristics (Fig. 5D). The calculated markers supported the annotation of other subclusters of T cell.

apFBs may suppress inflammatory immunity in the progression of DCM

To explore the role of apFB in regulating the immune microenvironment of DCM, we performed a communication analysis between fibroblast subpopulations and immune cells. The amount of intercellular communication in DCM was significantly increased (Fig. 6A, B). The interactions between apFB and CD4⁺T revealed that the count of signals received by CD4⁺T_{EX} and CD4⁺T_{reg} was nearly doubled in DCM (Fig. 6C). Compared with other fibroblasts, apFB was the only fibroblast that transmitted MHCII signaling to CD4⁺T_{EX} and CD4⁺T_{reg} via HLA-DRB1-CD4 (Fig. 6D, E). The corresponding communication probability of HLA-DRB1-CD4 between apFB and CD4⁺T was moderately strong compared with multiple L-R pairs between myeloid cells and CD4⁺T cells (Fig. 6F).

Furthermore, apFB may be incapable of activating CD4⁺T cells because it barely expressed co-stimulated molecules, including CD80, CD86, and CD40 (Fig. 6G). The upregulated L-R pairs from apFBs to CD4⁺T cells in DCM were investigated. The L-R pairs of TGF- β , MIF, IL-6, CXCL, CLEC, and CD46 signals were upregulated in DCM (Fig. 6H). According to this result, apFBs appeared to enhance the recruitment of CD4⁺T in DCM through MIF and CXCL pathway-related L-R pairs and might inhibit the activity of CD4⁺T_{EX} by secreting TGF- β , thereby attenuating its inflammatory factor secretion [32, 33]. The significant positive correlation between apFBs and T_{reg} cells in bulk RNA Seq data from 166 DCM patients further suggested the immunosuppressive potential of apFBs (Fig. 6I). Previous analysis suggested that IFN- γ response-related genes were enriched in apFBs and were associated with the acquisition of antigen-presenting phenotypes of fibroblasts. The pattern of the IFN-II signaling network was different between donor and DCM cells (Fig. 6J). Although CD4⁺T_{EX} and FB1 produce high levels of IFN- γ in DCM, the signal strength is decreased in DCM, whereas myeloid cells and B cells upregulate IFN-II signaling in DCM. This finding suggests that apFB-enhanced antigen presentation is primarily regulated by the myeloid cells in DCM. This potential crosstalk between apFBs and immune cells is summarized in Fig. 7.

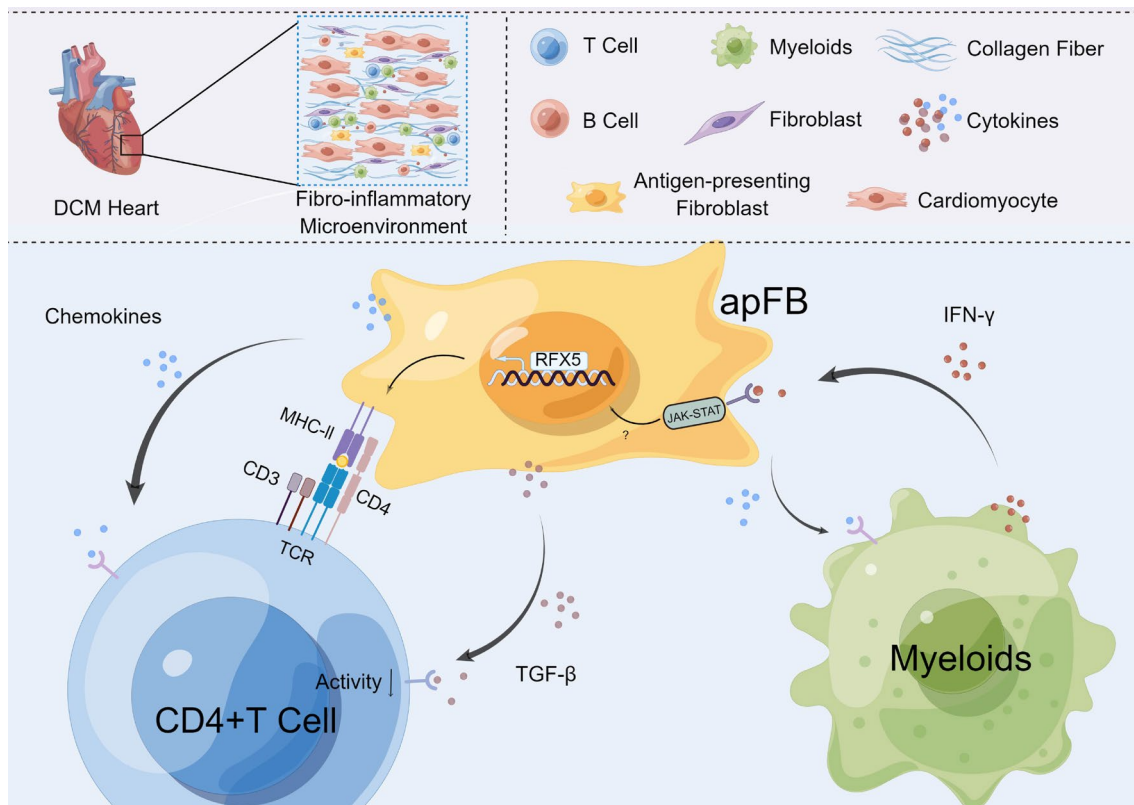


Fig. 7 Schematic illustration of intercellular crosstalk between apFBs and immune cells. The apFBs existing in the DCM heart may participate in the regulation of the fibro-inflammatory microenvironment

A prognostic prediction model based on apFB signature genes

The potential role of apFBs in clinical applications was investigated. Most of the apFB signature genes (TGFB2, FBLN1, CD74, IL6, HLA-DRB1, HLA-DRA, MIF, TGFB3, CXCL2) demonstrated an ideal diagnostic efficacy (each achieved an $AUC \geq 0.68$) (Figure S3), indicating that these genes had great potential to be the diagnostic indicators for DCM patients. The random forest algorithm (trees = 500) was subsequently used to pick the three most important prognostic genes (TGFB2, FBLN1, and CD74) from the mentioned signature genes (Fig. 8A, B). Adding the basic clinical factors of age and sex, a final nomogram prediction model for DCM prognosis was established (Fig. 8C). The calibration curve of this model was relatively close to the ideal curve, which indicates that the predicted results were consistent with the actual findings (Fig. 8D). The decision curve analysis (DCA) curve demonstrated that the nomogram had great net benefits for clinical use (Fig. 8E).

Discussion

The progression of DCM is characterized by ventricular remodeling and myocardial inflammation, and various cell types contribute significantly to these pathological processes. Fibroblasts have been regarded as the primary contributors to cardiac structural remodeling [34, 35]. In the present study, the GO enrichment results showed that fibroblasts in DCM exhibited increased extracellular matrix production and collagen synthesis. Immune cells in DCM presented an up-regulation of cytokine production, immune activation, and enhanced phagocytosis. These findings support the theory that DCM is associated with increased inflammation, which has been verified in previous studies [36, 37]. In addition, previous researchers indicated that increased angiogenesis occurs early during cardiac remodeling while it later transitions into capillary dysfunction and capillary loss [38, 39], and enhanced endothelial cell apoptosis was observed in heart failure patients [40]. Our results also demonstrated that endothelial cells exhibited upregulation of genes involved angiogenesis and the intrinsic apoptotic signaling pathway

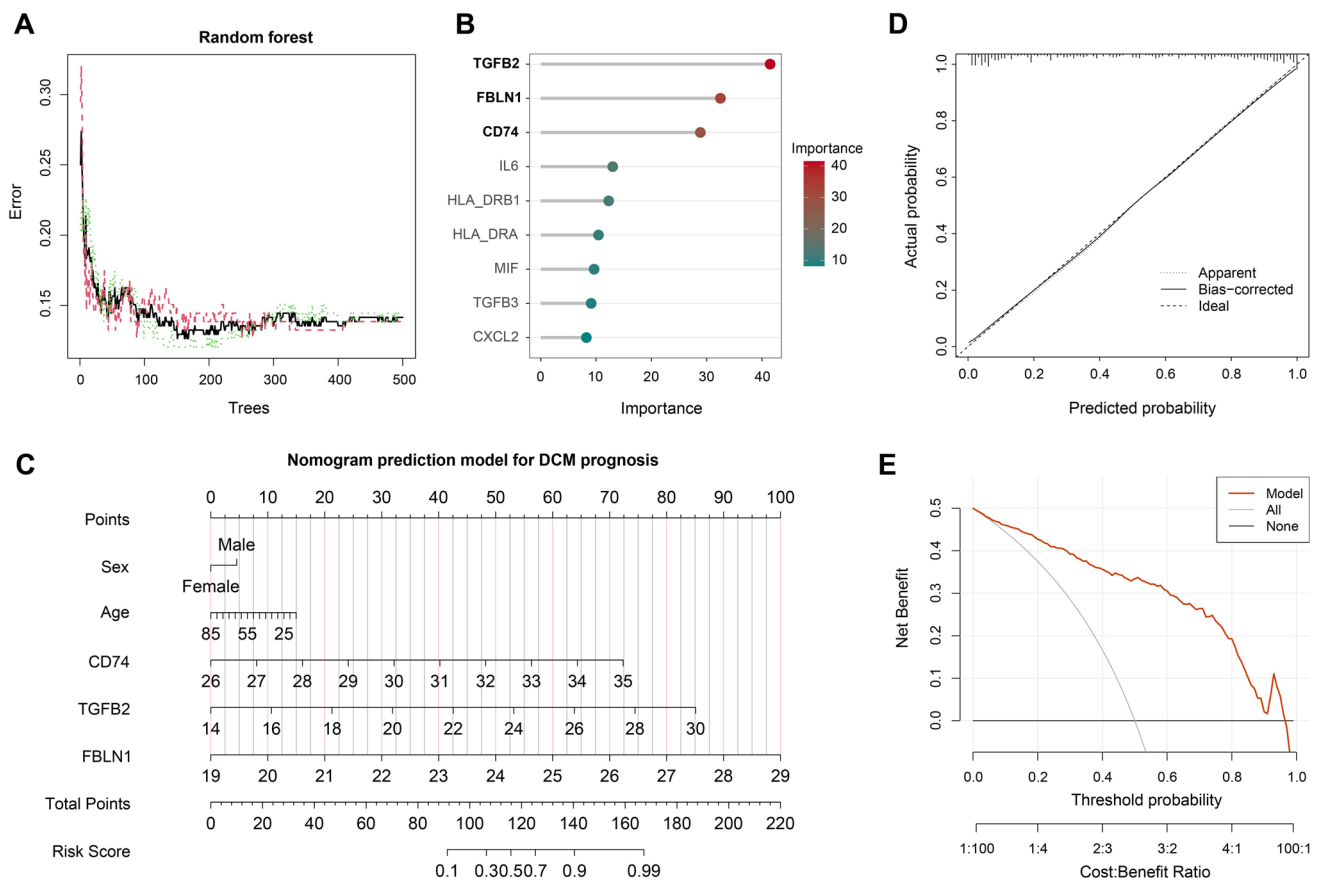


Fig. 8 Factor Selection for the Predictive Model, Calibration, and the Validation of the Nomogram. **A** Identification of the point with the smallest cross-validation error and finding the number of trees corresponding to it. **B** Importance score of 9 apFB signature genes. **C**

Nomogram prediction model for DCM prognosis. **D** Calibration curves of the nomogram prediction model. **E** Decision curve analysis of the nomogram

in response to DNA damage. These findings cooperatively suggested that endothelial cells may play a pivotal role in the pathogenesis and progression of DCM.

The changes of fibro-inflammatory microenvironment in DCM have attracted great attention in recent years, presenting that fibroblasts can promote inflammation in DCM, and immune cells can stimulate the proliferation and activation of fibroblasts [41, 42]. In our study, we noticed the upregulated expression of CD74 in DCM through DEG analysis of fibroblasts. According to this phenomenon we reasonably assumed that a subclass of fibroblasts expressing CD74 with antigen-presenting functions may exist in the adult heart. In previous studies, fibroblasts in human heart have not been reported to function as antigen-presenting cells. To test our speculation, we further re-clustered the fibroblasts, and 6 subpopulations were obtained. The results of marker gene GO enrichment indicated that the function of FB1, FB2, and FB3 exhibit a relatively similar profile, including extracellular matrix production, fiber synthesis, and wounding response. These 3 subpopulations exhibited a similar pattern to previous researches [43, 44]. The specific high

expression of ACTA2 suggested that typical myofibroblasts were also formed in DCM with enriched terms of response to wounding and cytoskeleton organization. In previous studies, an increase of myofibroblasts has been identified in HF [34, 35]. Consistent with these findings, we also found increased amounts of myofibroblasts in DCM hearts. Notably, apFBs, a subpopulation characterized by CD74, were obtained with the GO terms mainly related to antigen processing and presentation. The existence of apFBs was further validated in explanted DCM human heart via immunofluorescence-staining the MHCII molecule and PDGFR α . PDGFR α , a cell surface tyrosine kinase receptor for members of the platelet-derived growth factor family, is a specific marker protein of cardiac fibroblasts. Since MHCII molecules are also expressed on the cell membrane, apFB can be identified by recognizing the fluorescence colocalization signal of MHCII molecules and PDGFR α .

Despite being described decades ago in the rheumatoid arthritis model [45], a specific fibroblast capable of MHCII-mediated antigen-presenting within the tumor microenvironment [12, 46]. In previous researches, IFN- γ

and a hypoxic environment can contribute to apFBs formation [47]. In our study, we observed the upregulation of IFN- γ -responsive-related genes in apFBs. Besides, apFBs specifically expressed HLA-DR genes but no other MHC II molecule-related genes, suggesting that this transcriptional change could be induced by IFN- γ [48–50]. All of these indicate that apFBs may increase the expression of MHCII class molecules in DCM via IFN- γ -mediated mechanisms. We further revealed that the antigen presentation phenotype may be regulated by the increased activities of the transcription factor RFX5 and the JAK-STAT pathway.

Previous studies have shown that the activation of immune cells by antigen-presenting cells is dependent on the expression of costimulatory molecules [51]. To clarify the possible effecting mechanism of apFBs in DCM, we examined the expression of costimulatory molecules in apFBs, and found that apFBs does not express classical costimulatory molecules such as CD80, CD86, or CD40. In addition, we noticed that the L-R pairs CLEC2B-KLRB1, CD46-JAG1, and TGF- β -TGFR between apFBs and CD4⁺T cells upregulated in DCM. KLRB1 encodes the CD161 protein, and this receptor protein is expressed in some CD4⁺ T cells, working as a potential inhibitory receptor [52]; CD46-JAG1 has been reported to mediate the conversion of effector T cells to T_{reg} [53]; TGF- β , a pleiotropic cytokine known to play key roles in shaping the tumor microenvironment, including immunosuppression. The absence of expression of co-stimulatory molecules and the upregulation of expression of immunosuppressive L-R pairs suggest that apFBs may function as an immunosuppressor in DCM. This result was further verified using correlation analysis between apFB and T_{reg}. Furthermore, CXCL pathway-related L-R pairs were upregulated between apFB and CD4⁺T suggesting that apFBs enhanced the recruitment of immune cells in DCM. Combined with these results, we hypothesized that apFBs can recruit CD4⁺ T cells by secreting chemokines, then inhibit the recruited effector T cells by producing TGF- β and activating CD161 on CD4⁺ T cells, thereby inhibiting the immune activity of CD4⁺ T cells; concurrently, the conversion of effector T cells to T_{reg} was mediated via the CD46-JAG1 signaling axis. However, this series of speculations must be more rigorously investigated and verified.

At the end of this study, the diagnostic value of the apFB signature genes was assessed, and each of the top 9 genes had an AUC value \geq 0.68. A prognostic prediction model was developed based on the top 3 important prognostic genes, which showed an ideal predictive performance and clinical applicability. In the future, a larger sample size should be utilized in a multicenter randomized controlled clinical study to confirm its predicting effects and the related

clinical benefits. However, the established model was based on the perioperative data, and a comprehensive database of DCM that incorporates survival data and sequencing information need be constructed in the future.

Overall, our study provides novel information regarding fibroblast subpopulations. apFBs, a newly identified subpopulation in human heart, may suppress inflammatory immunity via several immunosuppressive ligands in DCM. This finding further enriches the understanding of the fibro-inflammatory microenvironment in DCM and may have potential therapeutic applications.

Conclusions

In conclusion, we performed a comprehensive single-cell transcriptome analysis to identify a novel lineage of fibroblasts characterized by the expression of MHCII genes, whose existence was validated in human heart tissues. The transcriptomic data suggest that the new identified phenotype could be induced by the activation of the transcription factor RFX5 and JAK-STAT pathway in response to IFN- γ . apFBs exhibited a potential inflammation suppression role in DCM, suggesting a novel therapeutic target of HF. These results could be validated in further cellular and animal experiments.

Conflict of interests

The authors declare that the research was conducted in the absence of any commercial or financial relationships that could be construed as a potential conflict of interest.

Supplementary Information The online version contains supplementary material available at <https://doi.org/10.1007/s11010-024-04939-9>.

Acknowledgements The authors thank Dr Peiran, Huang for helpful comments and suggestions regarding data analysis and display.

Author contributions XS and XF conceived and designed this study. XF, BJ, and K.H. contributed to data analysis, histological experiments, and the original draft. YW, XS, YW, SJ and LP. participated in writing- review and editing. All authors reviewed the final manuscript.

Funding This work was supported by the National Natural Science Foundation of China (82370377, 81601663), Natural Science Foundation of Shanghai (23ZR1408800), and the Natural Science Foundation of Hebei Province of China (C20200206025).

Data availability The sequencing data used in this study (GSE145154, GSE183852, and GSE141910) are available from the GEO database (<https://www.ncbi.nlm.nih.gov/geo/>). The code used in this study is available upon request by contacting the corresponding author.

Declarations

Competing interests The authors declare no competing interests.

References

- Kiadaliri AA (2018) Global, regional, and national incidence, prevalence, and years lived with disability for 354 diseases and injuries for 195 countries and territories, 1990–2017: a systematic analysis for the global burden of disease study 2017. *The Lancet* 392:1789–1858
- Weintraub RG, Semsarian C, Macdonald P (2017) Dilated cardiomyopathy. *The Lancet* 390:400–414
- Zeng C, Duan F, Hu J, Luo B, Huang B, Lou X, Sun X, Li H, Zhang X, Yin S (2020) NLRP3 inflammasome-mediated pyroptosis contributes to the pathogenesis of non-ischemic dilated cardiomyopathy. *Redox Biol* 34:101523
- Mizoguchi F, Slowikowski K, Wei K, Marshall JL, Rao DA, Chang SK, Nguyen HN, Noss EH, Turner JD, Earp BE (2018) Functionally distinct disease-associated fibroblast subsets in rheumatoid arthritis. *Nat Commun* 9:1–11
- Humeres C, Vivar R, Boza P, Munoz C, Bolivar S, Anfossi R, Osorio JM, Olivares-Silva F, Garcia L, Diaz-Araya G (2016) Cardiac fibroblast cytokine profiles induced by proinflammatory or profibrotic stimuli promote monocyte recruitment and modulate macrophage M1/M2 balance in vitro. *J Mol Cell Cardiol* 101:69–80
- Bansal SS, Ismahil MA, Goel M, Zhou G, Rokosh G, Hamid T, Prabhu SD (2019) Dysfunctional and proinflammatory regulatory T-lymphocytes are essential for adverse cardiac remodeling in ischemic cardiomyopathy. *Circulation* 139:206–221
- Bajpai G, Schneider C, Wong N, Bredemeyer A, Hulsmans M, Nahrendorf M, Epelman S, Kreisel D, Liu Y, Itoh A, Shankar TS, Selzman CH, Drakos SG, Lavine KJ (2018) The human heart contains distinct macrophage subsets with divergent origins and functions. *Nat Med* 24:1234–1245
- Rao M, Wang X, Guo G, Wang L, Chen S, Yin P, Chen K, Chen L, Zhang Z, Chen X, Hu X, Hu S, Song J (2021) Resolving the intertwining of inflammation and fibrosis in human heart failure at single-cell level. *Basic Res Cardiol* 116:55
- Wang L, Yu P, Zhou B, Song J, Li Z, Zhang M, Guo G, Wang Y, Chen X, Han L, Hu S (2020) Single-cell reconstruction of the adult human heart during heart failure and recovery reveals the cellular landscape underlying cardiac function. *Nat Cell Biol* 22:108–119
- Tallquist MD (2020) Cardiac fibroblast diversity. *Annu Rev Physiol* 82:63–78
- Nicin L, Abplanalp WT, Schanzer A, Sprengel A, John D, Mellettin H, Tombor L, Keuper M, Ullrich E, Klingel K, Dettmeyer RB, Hoffmann J, Akintuerk H, Jux C, Schranz D, Zeiher AM, Rupp S, Dimmeler S (2021) Single nuclei sequencing reveals novel insights into the regulation of cellular signatures in children with dilated cardiomyopathy. *Circulation* 143:1704–1719
- Elyada E, Bolisetty M, Laise P, Flynn WF, Courtois ET, Burkhart RA, Teinor JA, Belleau P, Biffi G, Lucito MS (2019) Cross-species single-cell analysis of pancreatic ductal adenocarcinoma reveals antigen-presenting cancer-associated fibroblasts. *Cancer Discov* 9:1102–1123
- Huang H, Wang Z, Zhang Y, Pradhan RN, Ganguly D, Chandra R, Murimwa G, Wright S, Gu X, Maddipati R, Muller S, Turley SJ, Brekken RA (2022) Mesothelial cell-derived antigen-presenting cancer-associated fibroblasts induce expansion of regulatory T cells in pancreatic cancer. *Cancer Cell* 9:3922
- Koenig AL, Shchukina I, Amrute J, Andhey PS, Zaitsev K, Lai L, Bajpai G, Bredemeyer A, Smith G, Jones C, Terrebonne E, Rentschler SL, Artyomov MN, Lavine KJ (2022) Single-cell transcriptomics reveals cell-type-specific diversification in human heart failure. *Nature Cardiovascular Research* 1:263–280
- Korsunsky I, Millard N, Fan J, Slowikowski K, Zhang F, Wei K, Baglaenko Y, Brenner M, LohRaychaudhuri P-rs (2019) Fast, sensitive and accurate integration of single-cell data with Harmony. *Nat methods* 16:1289–1296
- Zappia L, Oshlack A (2018) Clustering trees: a visualization for evaluating clusterings at multiple resolutions. *Gigascience*. <https://doi.org/10.1093/gigascience/giy083>
- Finak G, McDavid A, Yajima M, Deng J, Gersuk V, Shalek AK, Slichter CK, Miller HW, McElrath MJ, Prlic M (2015) MAST: a flexible statistical framework for assessing transcriptional changes and characterizing heterogeneity in single-cell RNA sequencing data. *Genome Biol* 16:1–13
- Kolberg L, Raudvere U, Kuzmin I, Vilo J, Peterson H (2020) gprofiler2—an R package for gene list functional enrichment analysis and namespace conversion toolset g: profiler. *F1000Res* 9:709. <https://doi.org/10.12688/f1000research.24956.1>
- Ashburner M, Ball CA, Blake JA, Botstein D, Butler H, Cherry JM, Davis AP, Dolinski K, Dwight SS, Eppig JT (2000) Gene ontology: tool for the unification of biology. *Nat Genet* 25:25–29
- Jassal B, Matthews L, Viteri G, Gong C, Lorente P, Fabregat A, Sidiropoulos K, Cook J, Gillespie M, Haw R (2020) The reactome pathway knowledgebase. *Nucleic Acids Res* 48:D498–D503
- Kanehisa M, Sato Y, Furumichi M, Morishima K, Tanabe M (2019) New approach for understanding genome variations in KEGG. *Nucleic Acids Res* 47:D590–D595
- Shao X, Taha IN, Clauser KR, Gao Y, Naba A (2020) MatrixDB: the ECM-protein knowledge database. *Nucleic Acids Res* 48:D1136–D1144
- Alvarez MJ, Shen Y, Giorgi FM, Lachmann A, Ding BB, Ye BH, Califano A (2016) Functional characterization of somatic mutations in cancer using network-based inference of protein activity. *Nat Genet* 48:838–847
- Holland CH, Tanevski J, Perales-Patón J, Gleixner J, Kumar MP, Mereu E, Joughin BA, Stegle O, Lauffenburger DA, Heyn H (2020) Robustness and applicability of transcription factor and pathway analysis tools on single-cell RNA-seq data. *Genome Biol* 21:1–19
- Jin S, Guerrero-Juarez CF, Zhang L, Chang I, Ramos R, Kuan C-H, Myung P, Plikus MV, Nie Q (2021) Inference and analysis of cell-cell communication using cell chat. *Nat Commun* 12:1–20
- Dobin A, Davis CA, Schlesinger F, Drenkow J, Zaleski C, Jha S, Batut P, Chaisson M, Gingeras TR (2013) STAR: ultrafast universal RNA-seq aligner. *Bioinformatics* 29:15–21
- Reimand J, Kull M, Peterson H, Hansen J, Vilo J (2007) g: Profiler—a web-based toolset for functional profiling of gene lists from large-scale experiments. *Nucleic Acids Res* 35:W193–W200
- Reith W, LeibundGut-Landmann S, Waldburger J-M (2005) Regulation of MHC class II gene expression by the class II transactivator. *Nat Rev Immunol* 5:793–806
- Zheng L, Qin S, Si W, Wang A, Xing B, Gao R, Ren X, Wang L, Wu X, Zhang J, Wu N, Zhang N, Zheng H, Ouyang H, Chen K, Bu Z, Hu X, Ji J, Zhang Z (2021) Pan-cancer single-cell landscape of tumor-infiltrating T cells. *Science* 374:abe6474
- Sun K, Xu R, Ma F, Yang N, Li Y, Sun X, Jin P, Kang W, Jia L, Xiong J (2022) scRNA-seq of gastric tumor shows complex intercellular interaction with an alternative T cell exhaustion trajectory. *Nat Commun* 13:1–19

31. Wherry EJ, Kurachi M (2015) Molecular and cellular insights into T cell exhaustion. *Nat Rev Immunol* 15:486–499
32. Chen W, Ten Dijke P (2016) Immunoregulation by members of the TGF β superfamily. *Nat Rev Immunol* 16:723–740
33. Veldhoen M, Hocking RJ, Atkins CJ, Locksley RM, Stockinger B (2006) TGF β in the context of an inflammatory cytokine milieu supports de novo differentiation of IL-17-producing T cells. *Immunity* 24:179–189
34. Weber KT, Díez J (2016) Targeting the cardiac myofibroblast secretome to treat myocardial fibrosis in heart failure. *Circ: Heart Fail* 9:e003315
35. Nagaraju CK, Robinson EL, Abdesselem M, Trenson S, Dries E, Gilbert G, Janssens S, Van Cleemput J, Rega F, Meyns B (2019) Myofibroblast phenotype and reversibility of fibrosis in patients with end-stage heart failure. *J Am Coll Cardiol* 73:2267–2282
36. Harding D, Chong MHA, Lahoti N, Bigogno CM, Prema R, Mohiddin SA et al (2023) Dilated cardiomyopathy and chronic cardiac inflammation: pathogenesis, diagnosis and therapy. *J Intern Med* 293(1):23–47
37. Immunomodulatory Cell Therapy Using α GalCer-Pulsed Dendritic Cells Ameliorates Heart Failure in a Murine Dilated Cardiomyopathy Model - PubMed [Internet]. [cited 2024 Jan 7]. Available from: <https://pubmed.ncbi.nlm.nih.gov/36268712/>
38. Gogiraju R, Bochenek ML, Schäfer K (2019) Angiogenic endothelial cell signaling in cardiac hypertrophy and heart failure. *Front Cardiovasc Med* 6:20
39. Shiojima I, Sato K, Izumiya Y, Schiekofer S, Ito M, Liao R et al (2005) Disruption of coordinated cardiac hypertrophy and angiogenesis contributes to the transition to heart failure. *J Clin Invest* 115(8):2108–2118
40. Gogiraju R, Xu X, Bochenek ML, Steinbrecher JH, Lehnart SE, Wenzel P et al (2015) Endothelial p53 deletion improves angiogenesis and prevents cardiac fibrosis and heart failure induced by pressure overload in mice. *J Am Heart Assoc* 4(2):e001770
41. Tucker W, Tucker B, Rye K-A, Ong KL (2022) Fibroblast growth factor 21 in heart failure. *Heart Fail Rev* 28:1–12
42. Bradshaw AD, DeLeon-Pennell KY (2020) T-cell regulation of fibroblasts and cardiac fibrosis. *Matrix Biol* 91:167–175
43. McLellan MA, Skelly DA, Dona MSI, Squiers GT, Farrugia GE, Gaynor TL et al (2020) High-resolution transcriptomic profiling of the heart during chronic stress reveals cellular drivers of cardiac fibrosis and hypertrophy. *Circulation* 142(15):1448–1463
44. Forte E, Skelly DA, Chen M, Daigle S, Morelli KA, Hon O et al (2020) Dynamic interstitial cell response during myocardial infarction predicts resilience to rupture in genetically diverse mice. *Cell Rep* 30(9):3149–3163.e6
45. Boots A, Wimmers-Bertens A, Rijnders A (1994) Antigen-presenting capacity of rheumatoid synovial fibroblasts. *Immunology* 82:268
46. Friedman G, Levi-Galibov O, David E, Bornstein C, Giladi A, Dadiani M, Mayo A, Halperin C, Pevsner-Fischer M, Lavon H (2020) Cancer-associated fibroblast compositions change with breast cancer progression linking the ratio of S100A4+ and PDPN+ CAFs to clinical outcome. *Nature Cancer* 1:692–708
47. Kerdidani D, Goudevenou K, Aerakis E (2020) Antigen-presenting fibroblasts sustain anti-tumour CD4+ T cells in situ via MHCIIp-TCR and C1q–C1qbp binding. *BioRxiv* 130(4):1492–1494. <https://doi.org/10.4049/jimmunol.130.4.1492>
48. Basham T, Merigan TC (1983) Recombinant interferon-gamma increases HLA-DR synthesis and expression. *J Immunol* 130:1492–1494
49. Alvaro-Gracia JM, Zvaifler NJ, Firestein GS (1990) Cytokines in chronic inflammatory arthritis. V. Mutual antagonism between interferon-gamma and tumor necrosis factor-alpha on HLA-DR expression, proliferation, collagenase production, and granulocyte macrophage colony-stimulating factor production by rheumatoid arthritis synoviocytes. *J clinical investigation* 86:1790–1798
50. Phillips R (2021) NK cells induce a pro-inflammatory phenotype in RA synovial fibroblasts. *Nat Rev Rheumatol* 17:645–645
51. Myers DR, Zikherman J, Roose JP (2017) Tonic signals: why do lymphocytes bother? *Trends Immunol* 38:844–857
52. Mathewson ND, Ashenberg O, Tirosh I, Gritsch S, Perez EM, Marx S, Jerby-Arnon L, Chanoch-Myers R, Hara T, Richman AR (2021) Inhibitory CD161 receptor identified in glioma-infiltrating T cells by single-cell analysis. *Cell* 184(1281–1298):e26
53. Le Friec G, Sheppard D, Whiteman P, Karsten CM, Shamoun SA-T, Laing A, Bugeon L, Dallman MJ, Melchionna T, Chillakuri C (2012) The CD46-jagged1 interaction is critical for human TH1 immunity. *Nat Immunol* 13:1213–1221

Publisher's Note Springer Nature remains neutral with regard to jurisdictional claims in published maps and institutional affiliations.

Springer Nature or its licensor (e.g. a society or other partner) holds exclusive rights to this article under a publishing agreement with the author(s) or other rightsholder(s); author self-archiving of the accepted manuscript version of this article is solely governed by the terms of such publishing agreement and applicable law.